Mass Determination of Missing Particles at High Energy Electron Positron Colliders

Qian-Fei Xiang (向仟飞)

Institute of High Energy Physics, CAS

USTC, Hefei, Aug 25, 2016

Outline

1. **Review of mass measurements**
   - Different mass measurement methods
2. **Edge variables, $(m_Y^{\rm edge}, m_N^{\rm edge})$**
   - Edge variables, $(m_Y^{\rm edge}, m_N^{\rm edge})$
   - Mass determination with realistic considerations
   - Results
3. **Conclusions**

Mass measurement

Matrix Element method Comparing statistical likelihood under different mass hypotheses.

Adv. High precision. The best way to determine mass once signal and background is clearly understood.

Disad. Do not perform well in the early stages when there remains some debate as to the nature of the model being fitted, and in particular when the distribution of the background is poorly understood.

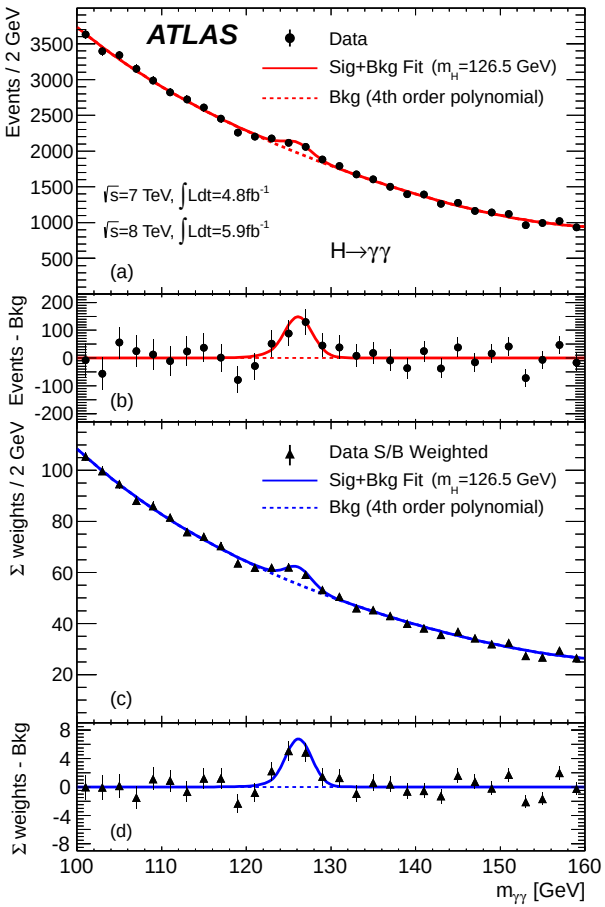

Mass measurement

Matrix Element method Comparing statistical likelihood under different mass hypotheses.

Adv. High precision. The best way to determine mass once signal and background is clearly understood.

Disad. Do not perform well in the early stages when there remains some debate as to the nature of the model being fitted, and in particular when the distribution of the background is poorly understood.

Kinematic methods Aiming at features of kinematic variables.

Adv. Few assumptions about the details of the underlying physical model (gauge groups, spins etc)

Disad. Low precision

See, review A. J. Barr and C. G. Lester, J. Phys. G37, 123001 (2010)

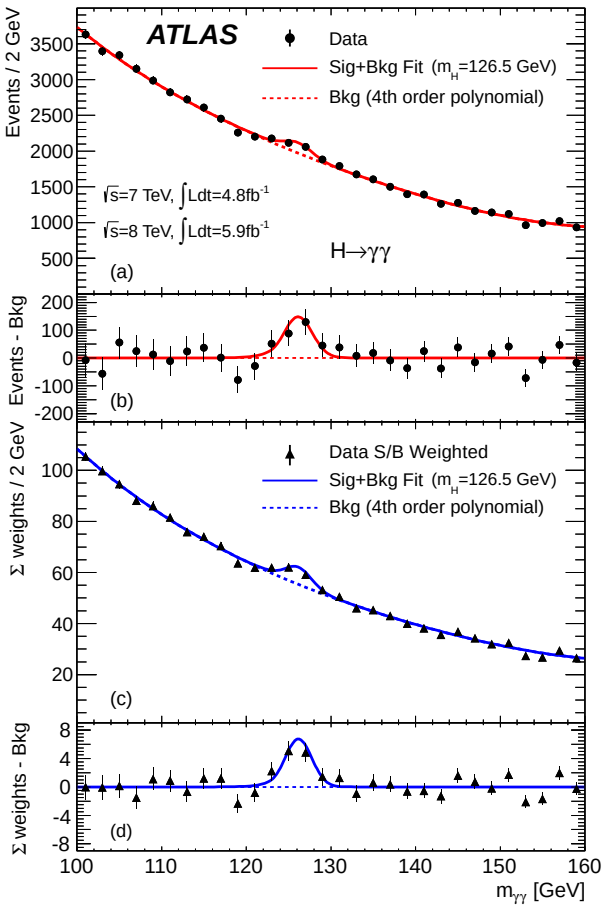

Endpoint methods

Endpoint methods use the kinematic edges of invariant mass distributions of the visible particles in a given cascade decay.

Example: dilepton topology

$$\tilde{\chi}_2^0 \to q l^\pm \tilde{l}^\mp \to q l^\pm l^\mp \tilde{\chi}_1^0$$

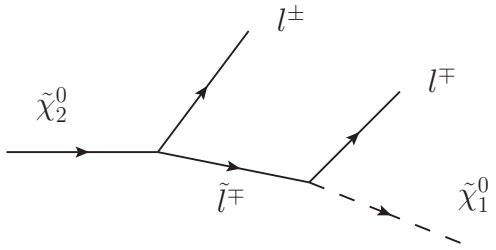

$$(m_{ll}^{max})^2 = \frac{(m^2_{\tilde{\chi}_2^0} - m^2_{\tilde{l}})(m^2_{\tilde{l}} - m^2_{\tilde{\chi}_1^0})}{m^2_{\tilde{\chi}_2^0}}$$

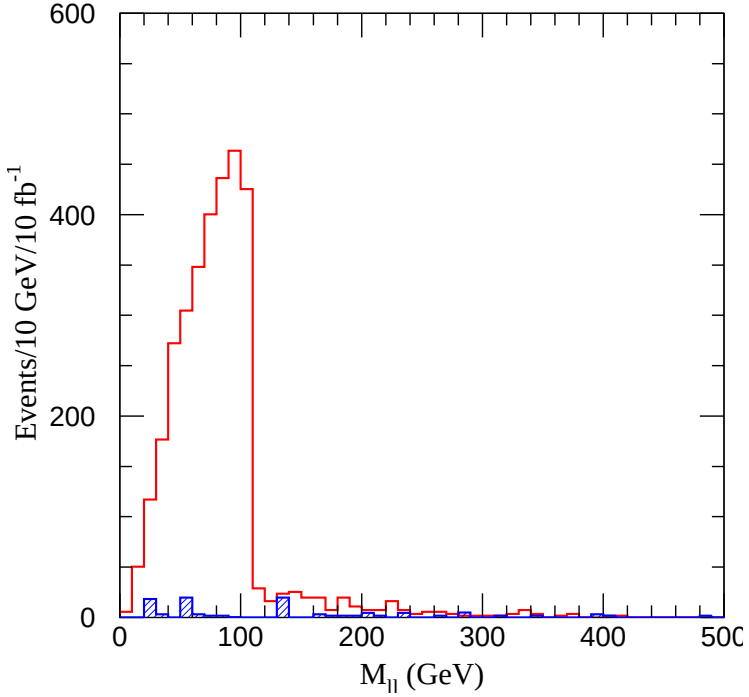

By combining several endpoints, the mass on invisible particle could be determined.

Different kinematic methods

- Endpoint methods
  B. K. Gjelsten, D. J. Miller, and P. Osland, JHEP 06, 015 (2005)
  D. J. Miller, P. Osland, and A. R. Raklev, JHEP 03, 034 (2006)
  M. Burns, K. Kong, K. T. Matchev, and M. Park, JHEP 10, 081 (2008)
- M_{T2} methods
  P. Meade and M. Reece, Phys. Rev. D74, 015010 (2006)
  C. Lester and A. Barr, JHEP 12, 102 (2007)
  M. Burns, K. Kong, K. T. Matchev, and M. Park, JHEP 03, 143 (2009)
- Polynomial methods
  H.-C. Cheng, D. Engelhardt, J. F. Gunion et al., Phys. Rev. Lett. 100, 252001 (2008)
  H.-C. Cheng, J. F. Gunion, Z. Han, and B. McElrath, Phys. Rev. D80, 035020 (2009)
- Hybrid methods
  H.-C. Cheng and Z. Han, JHEP 12, 063 (2008)
  H.-C. Cheng, J. F. Gunion, Z. Han et al., JHEP 12, 076 (2007)
- Others
  K. Agashe, R. Franceschini, D. Kim et al., Phys. Dark Univ. 2, 72 (2013)
  K. Agashe, R. Franceschini, and D. Kim, JHEP 11, 059 (2014)
- ……

Kinematic equations

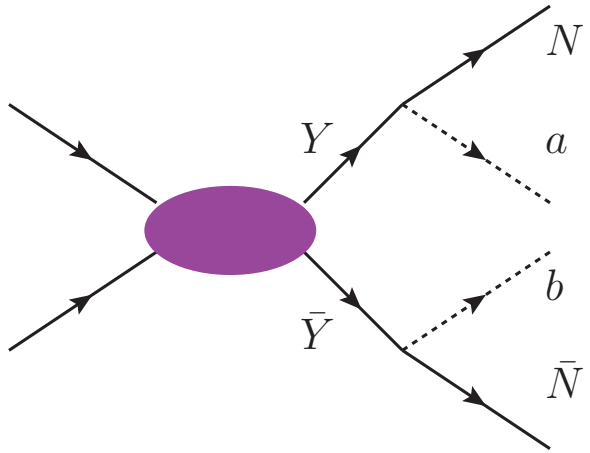

$$Y \to a(p_a) + N(k_1)$$

$$\bar{Y} \to b(p_b) + \bar{N}(k_2)$$

There are 8 unknowns in all:

$$k_1^\mu, \qquad k_2^\mu$$

Apparently, there are only 6 kinematic equations:

$$q^\mu = p_a^\mu + p_b^\mu + k_1^\mu + k_2^\mu$$

$$k_1^2 = k_2^2$$

$$(p_a + k_1)^2 = (p_b + k_2)^2$$

Kinematic equations

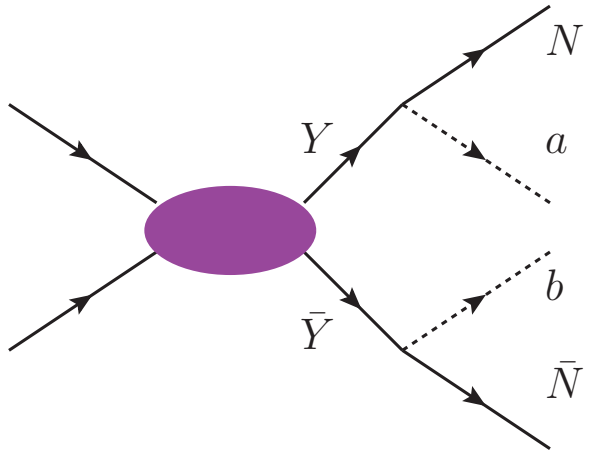

$$Y \to a(p_a) + N(k_1)$$

$$\bar{Y} \to b(p_b) + \bar{N}(k_2)$$

There are 8 unknowns in all:

$$k_1^\mu, \qquad k_2^\mu$$

Apparently, there are only 6 kinematic equations:

$$q^\mu = p_a^\mu + p_b^\mu + k_1^\mu + k_2^\mu$$

$$k_1^2 = k_2^2 = m_N^2$$

$$(p_a + k_1)^2 = (p_b + k_2)^2 = m_Y^2$$

By adding 2 trial masses, there are 8 equations and 8 variables, these equations are solvable.

Solvable region

Signal process: $e^+e^- \to \tilde{\mu}_R^+\tilde{\mu}_R^- \to \mu^+\mu^-\tilde{\chi}_1^0\tilde{\chi}_1^0$.
Solvable region given by one event.

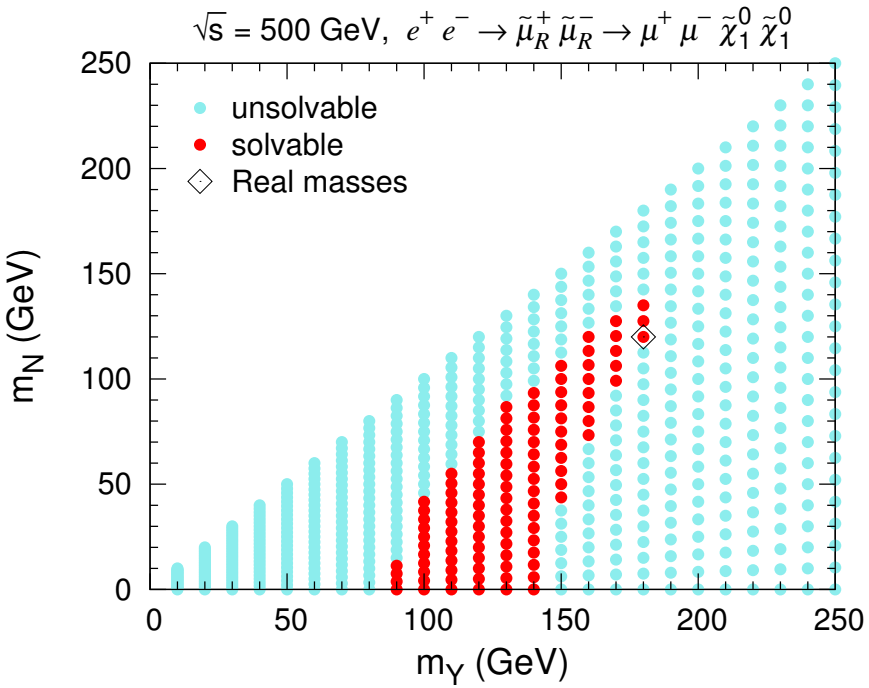

Theoretically, solvable region will always contain the real masses.

Solvable probabilities

Solvable probabilities for different values of (m_Y, m_N). The empty diamonds denote the real values.

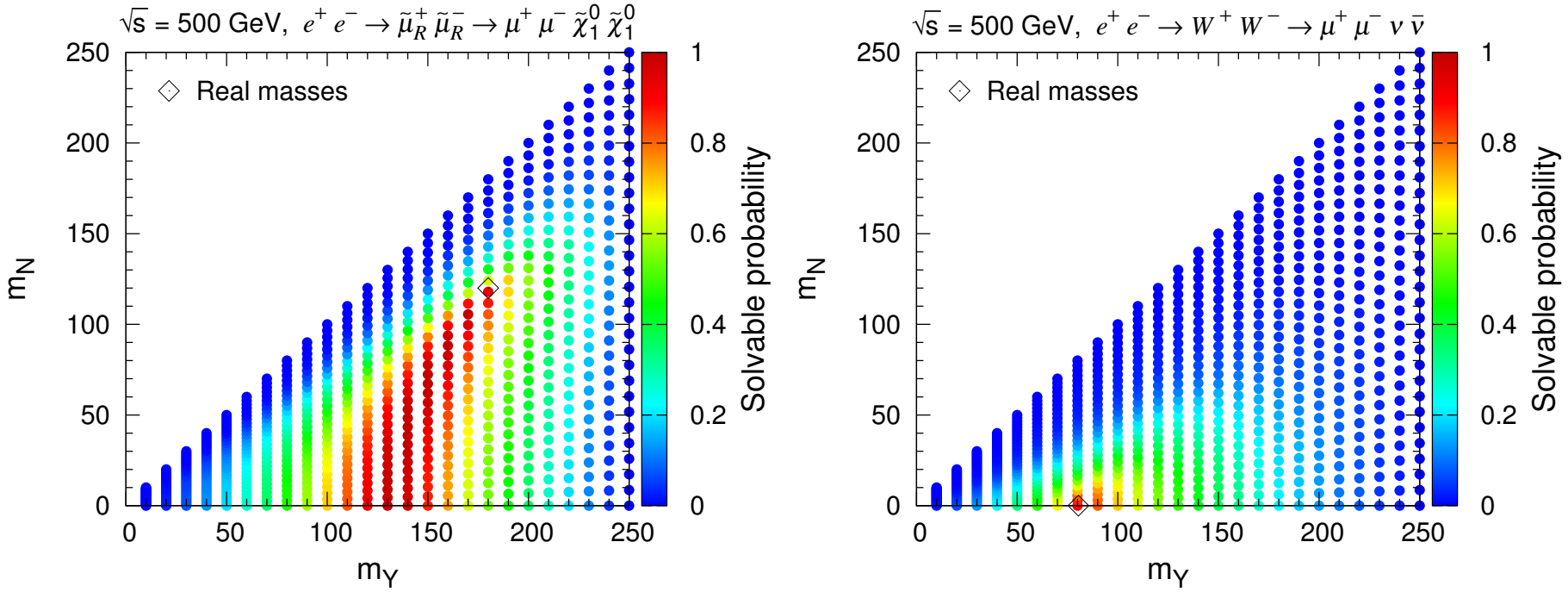

The real values of (m_Y, m_N) locate at the edge of the region with large solvable probabilities

$m_Y^{\rm edge}$ and $m_N^{\rm edge}$

$(m_Y^{\rm edge}, m_N^{\rm edge})$ is the point in solvable region with the largest distance from the origin (0, 0)

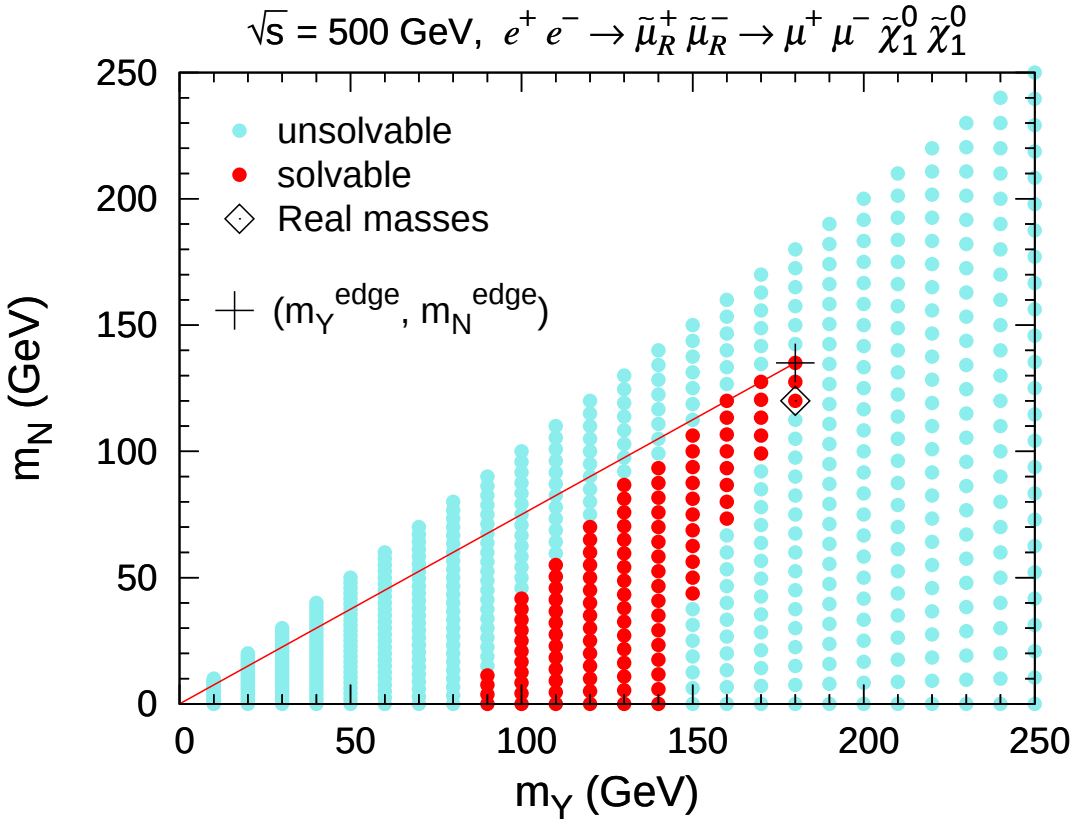

2D distributions of m_Y^{edge} and m_N^{edge}

Using 500 events, we get 500 m_Y^{edge} and m_N^{edge}, and then plot in the m_Y^{edge}-m_N^{edge} plane.

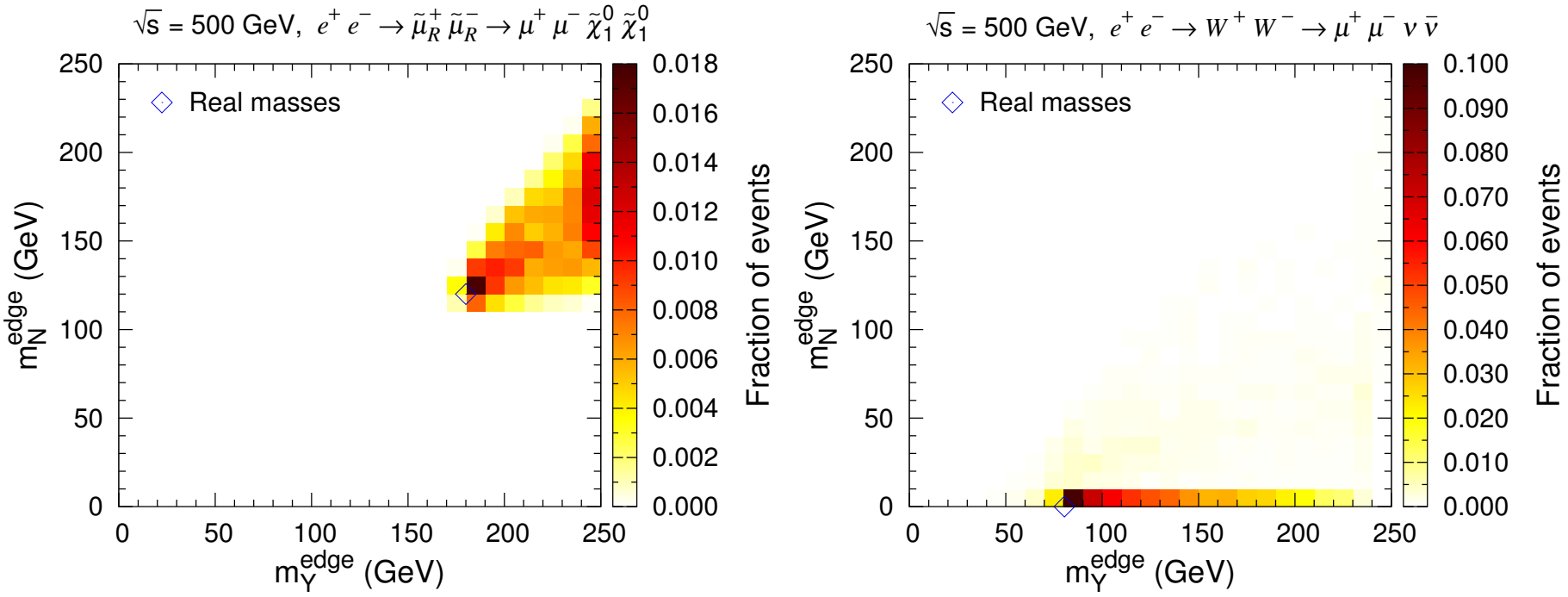

A peak structure is located at the vicinity of the real mass point.

1D distributions $m_Y^{\rm edge}$ and $m_N^{\rm edge}$

Project the 2D distributions to $m_Y^{\rm edge}$ and $m_N^{\rm edge}$

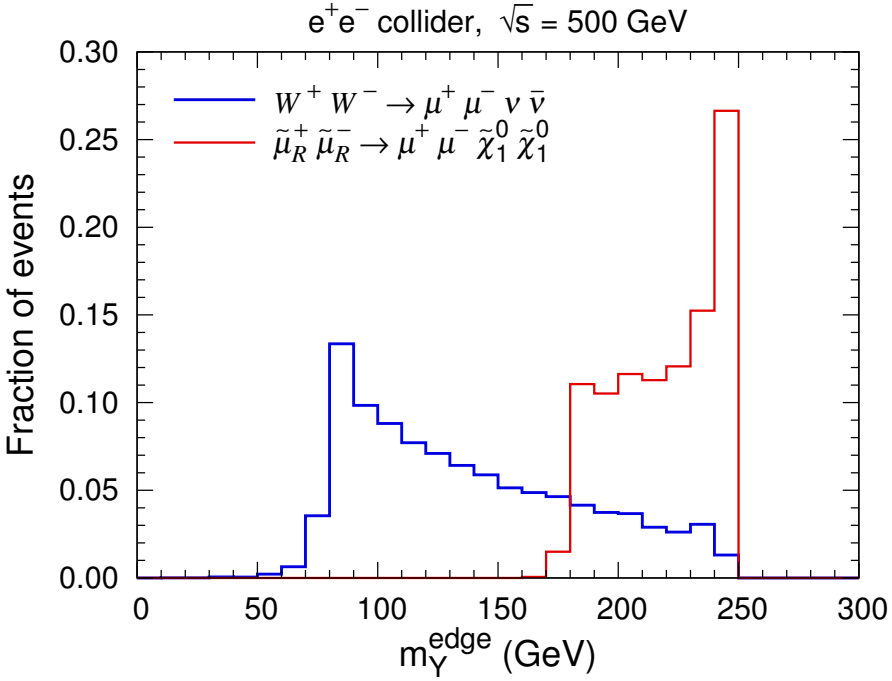

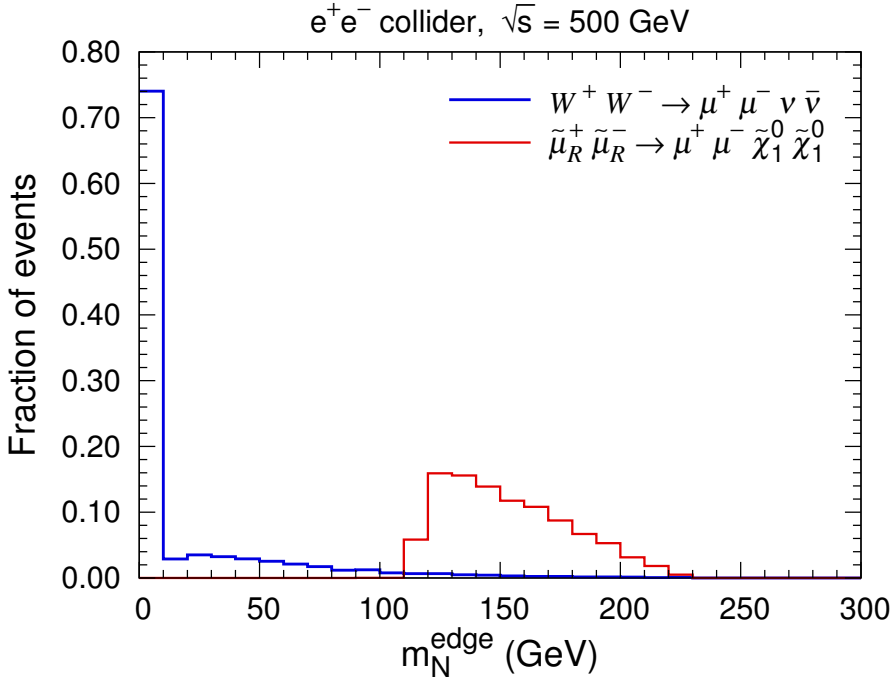

m_Y and m_N are lower endpoints of the $m_Y^{\rm edge}$ and $m_N^{\rm edge}$ distributions.

Fast detector simulations

We use Delphes 3 to carry out a fast detection.

In order to simulate the detector of high energy electron-positron colliders, We adopt the Delphes card adapted for ILD.

Fast detector simulations

We use Delphes 3 to carry out a fast detection.

In order to simulate the detector of high energy electron-positron colliders, We adopt the Delphes card adapted for ILD.

The main background is $e^+e^- \to \mu^+\mu^-\bar{\nu}_l\nu_l$, which including production through WW and ZZ and γZ.
We also consider the background$e^+e^- \to \mu^+\mu^-$ and $e^+e^- \to \tau^+\tau^-$.

Fast detector simulations

We use Delphes 3 to carry out a fast detection.

In order to simulate the detector of high energy electron-positron colliders, We adopt the Delphes card adapted for ILD.

The main background is $e^+e^- \to \mu^+\mu^-\bar{\nu}_l\nu_l$, which including production through WW and ZZ and γZ.
We also consider the background$e^+e^- \to \mu^+\mu^-$ and $e^+e^- \to \tau^+\tau^-$.

For illustration, we choose three BMPs with $(m_{\tilde{\mu}_R}, m_{\tilde{\chi}_1^0})$ equal $(135\ \text{GeV}, 45\ \text{GeV})$, $(175\ \text{GeV}, 115\ \text{GeV})$, and $(175\ \text{GeV}, 155\ \text{GeV})$.

Cuts and cut efficiency

	4body	WW	γZ	ZZ	$\mu^+\mu^-$	$\tau^+\tau^-$	BP1	BP2	BP3
Parton level	96.08	61.79	1.89	4.89	419.70	419.91	59.64	36.05	36.05
lepton	65.71	47.50	1.18	3.73	369.67	9.99	47.29	28.42	20.23
$\not{E}$	64.83	46.66	1.18	3.72	9.57	9.41	47.09	28.18	19.18
$\Delta\phi$	23.55	12.21	0.73	2.70	~ 0	~ 0	22.00	16.65	9.81
$m_{\mu\mu}$	5.34	2.76	0.58	0.18	~ 0	~ 0	17.38	14.01	9.72
cut efficiency	5.55	-	-	-	-	-	29.15	38.86	26.95

Cuts and cut efficiency

	4body	WW	γZ	ZZ	$\mu^+\mu^-$	$\tau^+\tau^-$	BP1	BP2	BP3
Parton level	96.08	61.79	1.89	4.89	419.70	419.91	59.64	36.05	36.05
lepton	65.71	47.50	1.18	3.73	369.67	9.99	47.29	28.42	20.23
$\not{E}$	64.83	46.66	1.18	3.72	9.57	9.41	47.09	28.18	19.18
$\Delta\phi$	23.55	12.21	0.73	2.70	~ 0	~ 0	22.00	16.65	9.81
$m_{\mu\mu}$	5.34	2.76	0.58	0.18	~ 0	~ 0	17.38	14.01	9.72
cut efficiency	5.55	-	-	-	-	-	29.15	38.86	26.95

- Lepton requirement: Two isolated μ with $p_T > 10$ GeV and $|\eta| < 2.5$, no e with $p_T > 10$ GeV and $|\eta| < 2.5$.

Cuts and cut efficiency

	4body	WW	γZ	ZZ	$\mu^+\mu^-$	$\tau^+\tau^-$	BP1	BP2	BP3
Parton level	96.08	61.79	1.89	4.89	419.70	419.91	59.64	36.05	36.05
lepton	65.71	47.50	1.18	3.73	369.67	9.99	47.29	28.42	20.23
$\not{E}$	64.83	46.66	1.18	3.72	9.57	9.41	47.09	28.18	19.18
$\Delta\phi$	23.55	12.21	0.73	2.70	~ 0	~ 0	22.00	16.65	9.81
$m_{\mu\mu}$	5.34	2.76	0.58	0.18	~ 0	~ 0	17.38	14.01	9.72
cut efficiency	5.55	-	-	-	-	-	29.15	38.86	26.95

- Lepton requirement: Two isolated μ with $p_T > 10$ GeV and $|\eta| < 2.5$, no e with $p_T > 10$ GeV and $|\eta| < 2.5$.
- $\not{E} > 5$ GeV

Cuts and cut efficiency

	4body	WW	γZ	ZZ	$\mu^+\mu^-$	$\tau^+\tau^-$	BP1	BP2	BP3
Parton level	96.08	61.79	1.89	4.89	419.70	419.91	59.64	36.05	36.05
lepton	65.71	47.50	1.18	3.73	369.67	9.99	47.29	28.42	20.23
$\not{E}$	64.83	46.66	1.18	3.72	9.57	9.41	47.09	28.18	19.18
$\Delta\phi$	23.55	12.21	0.73	2.70	~ 0	~ 0	22.00	16.65	9.81
$m_{\mu\mu}$	5.34	2.76	0.58	0.18	~ 0	~ 0	17.38	14.01	9.72
cut efficiency	5.55	-	-	-	-	-	29.15	38.86	26.95

- Lepton requirement: Two isolated μ with $p_T > 10$ GeV and $|\eta| < 2.5$, no e with $p_T > 10$ GeV and $|\eta| < 2.5$.
- $\not{E} > 5$ GeV
- $\Delta\phi < 2.4$ $\mu^+\mu^-$ and $\tau^+\tau^-$ are produced back-to-back
- $m_{\mu\mu}$ Discard the events with $|m_{\mu\mu} - m_Z| < 10$ GeV; veto the events with $m_{\mu\mu} > 220$ GeV; reject the events for $m_{\mu\mu} < 10$ GeV in order to remove events from the quarkonium decay.

Cuts and cut efficiency

	4body	WW	γZ	ZZ	$\mu^+\mu^-$	$\tau^+\tau^-$	BP1	BP2	BP3
Parton level	96.08	61.79	1.89	4.89	419.70	419.91	59.64	36.05	36.05
lepton	65.71	47.50	1.18	3.73	369.67	9.99	47.29	28.42	20.23
$\not{E}$	64.83	46.66	1.18	3.72	9.57	9.41	47.09	28.18	19.18
$\Delta\phi$	23.55	12.21	0.73	2.70	~ 0	~ 0	22.00	16.65	9.81
$m_{\mu\mu}$	5.34	2.76	0.58	0.18	~ 0	~ 0	17.38	14.01	9.72
cut efficiency	5.55	-	-	-	-	-	29.15	38.86	26.95

- Lepton requirement: Two isolated μ with $p_T > 10$ GeV and $|\eta| < 2.5$, no e with $p_T > 10$ GeV and $|\eta| < 2.5$.
- $\not{E} > 5$ GeV
- $\Delta\phi < 2.4$ $\mu^+\mu^-$ and $\tau^+\tau^-$ are produced back-to-back
- $m_{\mu\mu}$ Discard the events with $|m_{\mu\mu} - m_Z| < 10$ GeV; veto the events with $m_{\mu\mu} > 220$ GeV; reject the events for $m_{\mu\mu} < 10$ GeV in order to remove events from the quarkonium decay.

Cuts and cut efficiency

	4body	WW	γZ	ZZ	$\mu^+\mu^-$	$\tau^+\tau^-$	BP1	BP2	BP3
Parton level	96.08	61.79	1.89	4.89	419.70	419.91	59.64	36.05	36.05
lepton	65.71	47.50	1.18	3.73	369.67	9.99	47.29	28.42	20.23
$\not{E}$	64.83	46.66	1.18	3.72	9.57	9.41	47.09	28.18	19.18
$\Delta\phi$	23.55	12.21	0.73	2.70	~ 0	~ 0	22.00	16.65	9.81
$m_{\mu\mu}$	5.34	2.76	0.58	0.18	~ 0	~ 0	17.38	14.01	9.72
cut efficiency	5.55	-	-	-	-	-	29.15	38.86	26.95

- Lepton requirement: Two isolated μ with $p_T > 10$ GeV and $|\eta| < 2.5$, no e with $p_T > 10$ GeV and $|\eta| < 2.5$.
- $\not{E} > 5$ GeV
- $\Delta\phi < 2.4$ $\mu^+\mu^-$ and $\tau^+\tau^-$ are produced back-to-back
- $m_{\mu\mu}$ Discard the events with $|m_{\mu\mu} - m_Z| < 10$ GeV; veto the events with $m_{\mu\mu} > 220$ GeV; reject the events for $m_{\mu\mu} < 10$ GeV in order to remove events from the quarkonium decay.

Scatter plot

Scatter plot of m_Y^{edge} and m_N^{edge} for SM backgrounds and several BMPs, assuming 5,000 events for each process.

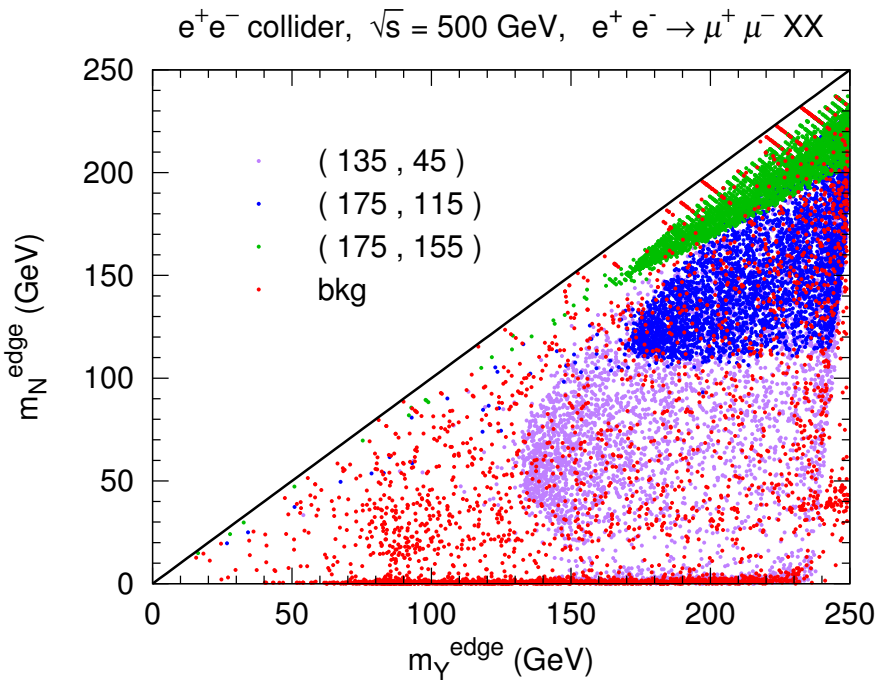

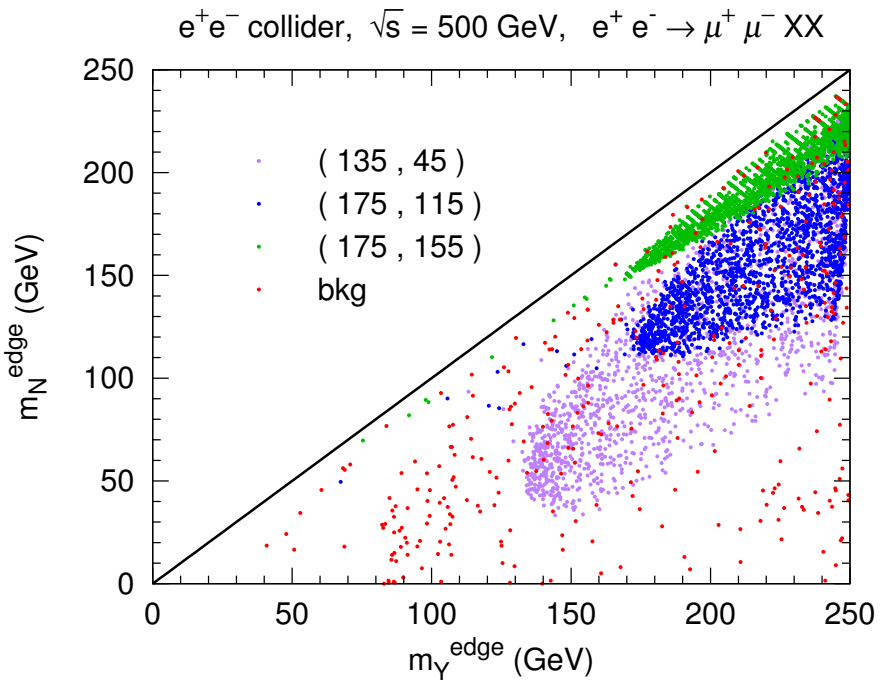

- (m_Y^{edge}, m_N^{edge}) distributions of backgrounds spread in the whole region.
- The distributions of signals are bounded by $m_{\tilde{\mu}_R}$ and $m_{\tilde{\chi}_1^0}$.
- These distributions can be used to discriminate signals and backgrounds.

Methods to determine the masses

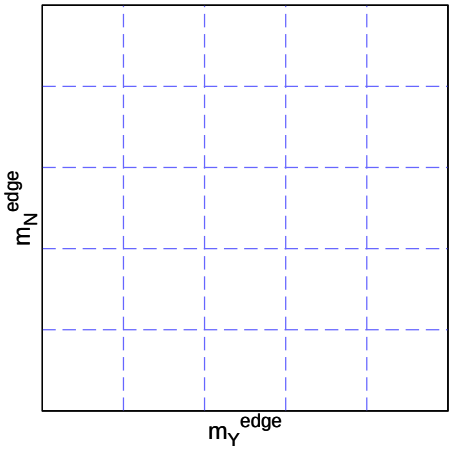

- Divide the $m_Y^{\rm edge} - m_N^{\rm edge}$ plane into many grids.

Methods to determine the masses

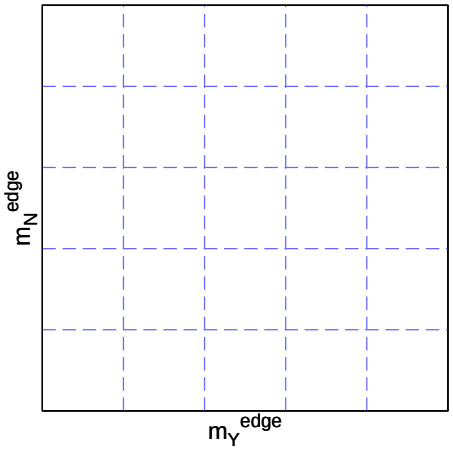

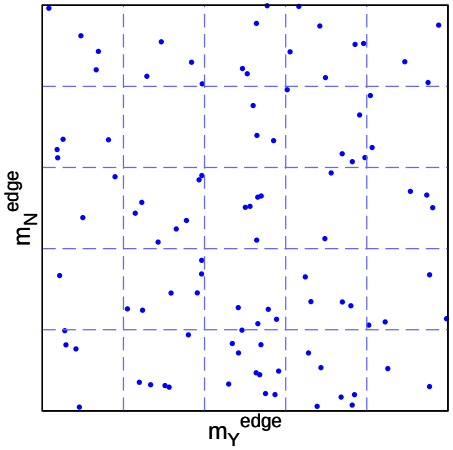

- Divide the $m_Y^{\rm edge} - m_N^{\rm edge}$ plane into many grids.
- Count the number of $(m_Y^{\rm edge}, m_N^{\rm edge})$ in each grid.

Methods to determine the masses

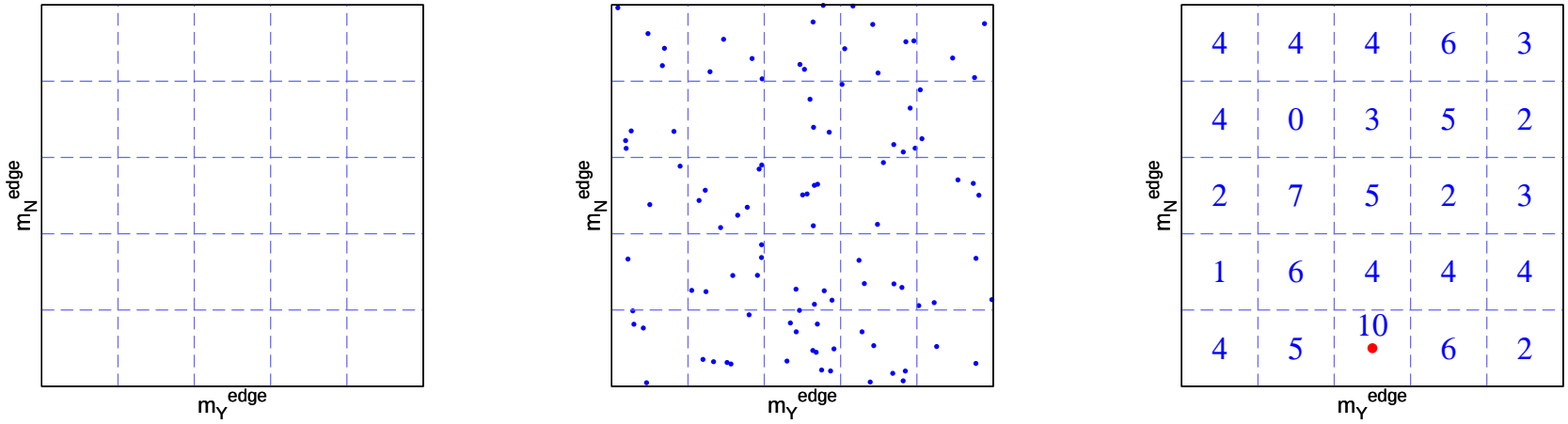

- Divide the $m_Y^{\rm edge} - m_N^{\rm edge}$ plane into many grids.
- Count the number of $(m_Y^{\rm edge}, m_N^{\rm edge})$ in each grid.
- Find the grid with largest number, and use the center of this grid to represent the m_Y and m_N

2D distributions of (m_Y^{edge}, m_N^{edge})

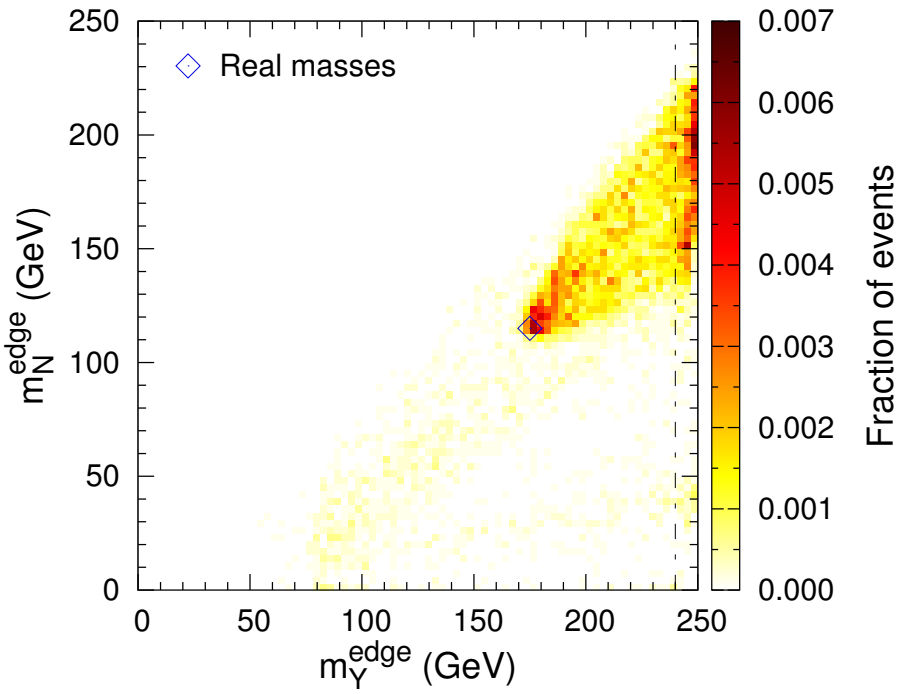

Problems

- The grids close to $m_Y^{edge} \sim \sqrt{s}/2$ have large density.
- Misidentify the grid with largest density.

Strategy for extracting m_Y and m_N

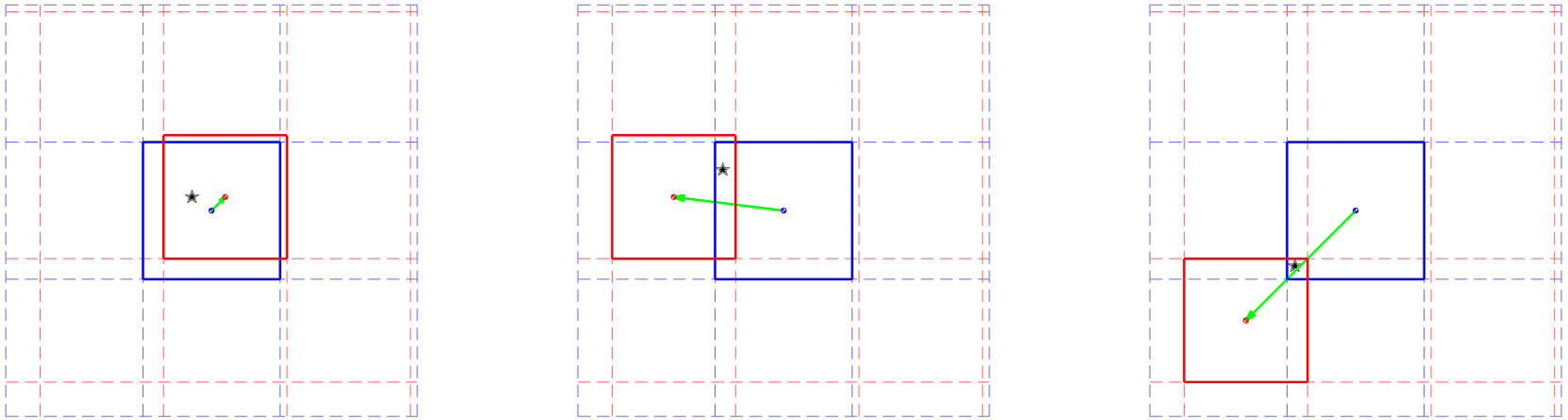

In two successive step, we require:

$$\sqrt{(m_{\rm Y}^{j+1} - m_{\rm Y}^{j})^2 + (m_{\rm N}^{j+1} - m_{\rm N}^{j})^2} \lesssim \sqrt{2} L_j$$

where $m_{\rm Y,N}^{j}$ ($m_{\rm Y,N}^{j+1}$) is the searched mass in j-th ($(j+1)$-th) step, and L_j is the width of grid in j-th step.
When this inequation is violation, we get the mass m_Y^j and m_N^j.

Illustraion of extracting m_Y and m_N

- Divide the m_Y-m_N into grids with witdth $L = 3$ GeV.
- Decrease the grid width L by increasing the grids number in the m_Y-m_N.

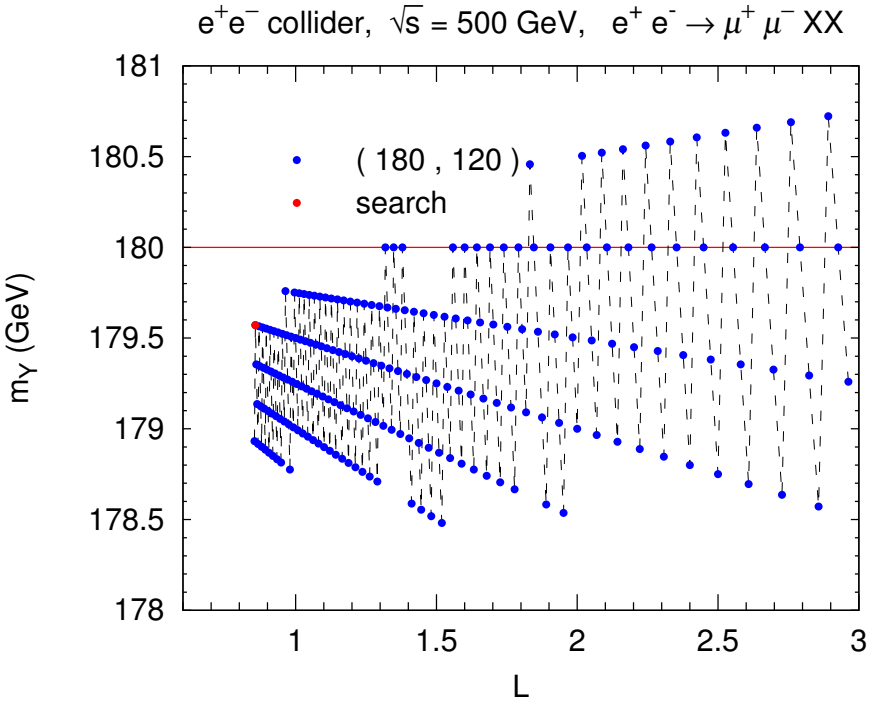

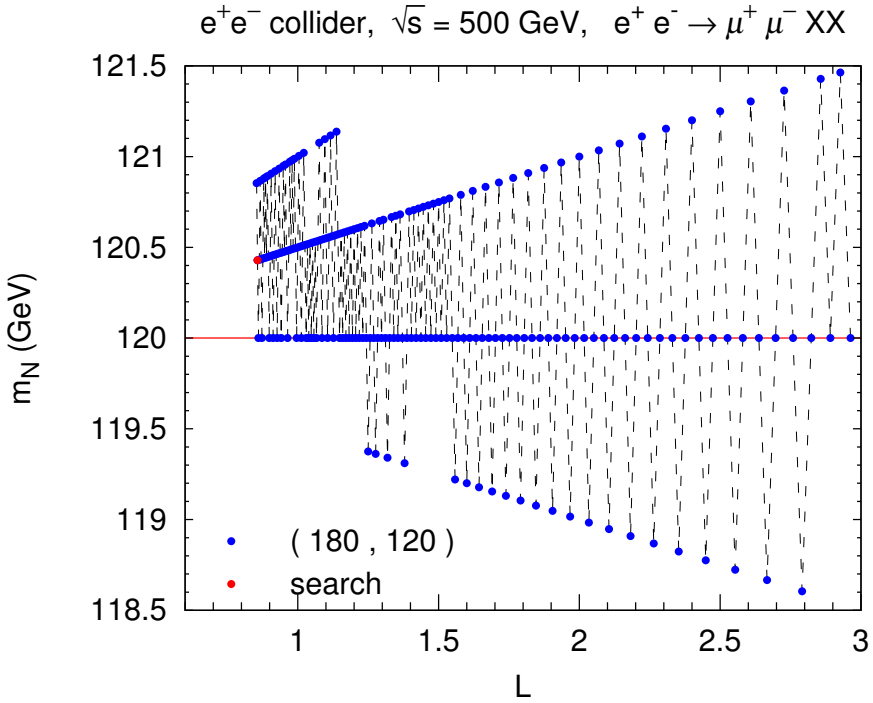

For the BMP (180,120), we get (179.6, 120.4), error is smaller than 0.5 GeV.

Results

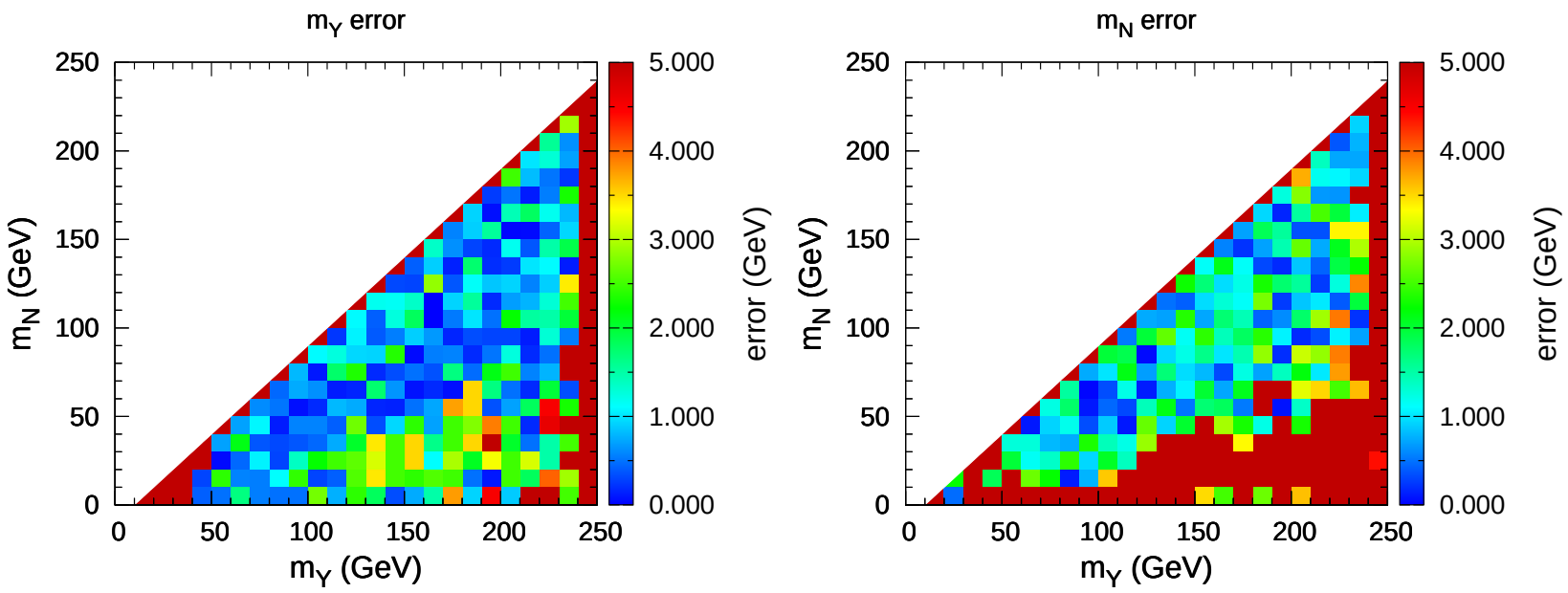

For many (m_Y, m_N), the errores of $m_Y(m_N)$ are smaller than 2 GeV(2.5 GeV)

Three blind regions:

- $m_Y \gtrsim 100$ GeV and $m_N \lesssim 50$ GeV. the real mass is not located at the edge of solvable region.
- $m_Y \sim 250$ GeV, production threshold
- $m_Y \sim m_N$, leptons too soft

Conclusions

- We proposed two new variables, $(m_Y^{\rm edge}, m_N^{\rm edge})$ and consider the masses determination in realistic situations.
- $(m_Y^{\rm edge}, m_N^{\rm edge})$ develop a peak structure at the vicinity of real masses, which can be used to discriminate signals from backgrounds.
- With an integrated luminosity of 200 $\rm fb^{-1}$, the error of m_Y (m_N) is less than 2.0 GeV (2.5 GeV) when $m_N \gtrsim 50$ GeV. There are three blind regions.

Thank you !